

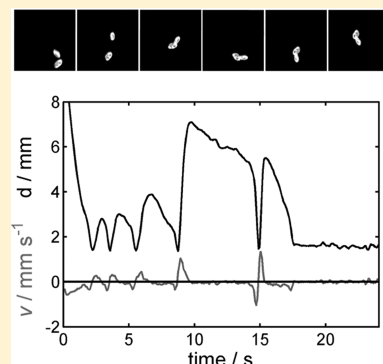
Motion and Interaction of Aspirin Crystals at Aqueous–Air Interfaces

Tamás Bánsági, Jr., Magdalena M. Wrobel, Stephen K. Scott, and Annette F. Taylor*

School of Chemistry, University of Leeds, Woodhouse Lane, Leeds LS2 9JT, United Kingdom

S Supporting Information

ABSTRACT: Small-molecule amphiphiles such as aspirin have unique properties arising from a combination of an aromatic hydrophobic part and a hydrophilic part. We show that crystals of aspirin are capable of generating convective flows at the air–aqueous interface from both Marangoni effects (through weak surface activity) and capillarity (surface deformations). The flow-driven motion of millimeter-sized crystals was found to depend on the presence of other ions in solution as well as the distance and orientation of the crystals. The interactions lead to the formation of groups of two or more crystals that also underwent motion. The convective flows created by small amphiphile crystals might be exploited in the dynamic self-organization of particles at interfaces.



■ INTRODUCTION

Processes occurring at interfaces, where intermolecular forces play a vital role, are important across a wide range of disciplines including materials science and the pharmaceutical sciences.^{1,2} Interfacial water has a relatively high surface tension arising from the loss of hydrogen-bonding neighbors of molecules at the surface compared with molecules in the bulk. Although the surface of water is a dynamic environment,^{3–5} it can act like an elastic membrane and support dense, hydrophobic objects by surface-tension-related (or surface-energy-related) forces.⁶ Small objects are able to move and interact on the surface of water as a result of Marangoni effects:⁷ the flow of liquid driven by surface tension gradients caused by local differences in chemical composition or temperature. The autonomous motion of camphor scrapings,⁸ oil or water droplets,^{9–12} and even some insects¹³ is achieved by chemically induced surface tension gradients. Marangoni flows have been exploited for the self-organization of millimeter-sized particles into moving swarms¹⁴ and nanoparticles into microscale structures.¹⁵

Another type of surface flow, capillary interactions, arises as a result of overlapping surface deformations from particles trapped at interfaces.¹⁶ Capillary interactions have been used for the dynamic self-assembly of catalytic particles, polymer microparticles, and protein globules.^{17–19} In 2D, similar capillary profiles, either hydrophilic–hydrophilic (positive menisci) or hydrophobic–hydrophobic (negative menisci), lead to attractive interactions that pull objects together. Unlike profiles (hydrophilic–hydrophobic) lead to repulsive interactions. The term capillary bond²⁰ has been employed to compare capillary interactions to van der Waals forces, although they typically act over greater distances (millimeters).²¹

We show that crystals of a small-molecule amphiphile, aspirin (*o*-acetylsalicylic acid), undergo autonomous motion and interactions at the air–water interface generated by a

combination of Marangoni effects, arising from surface activity, and capillarity (surface deformations). The motion is influenced by the addition of other ions that alter the surface tension; translational, rotational, and intermittent motion is observed, and motion ceases outside a bounded range of surface tensions. The complex surface flows generated by the organic crystals can lead to the formation of clusters of two or more crystals in specific orientations that also undergo motion.

Small-molecule amphiphiles consisting of hydrophobic benzene rings with hydrophilic side groups, such as acetylsalicylic acid, are weakly surface active and have hydrotropic properties: they aid in the solubilization of hydrophobic molecules.²² They are widely used in industry in drug formulations and cleaning and care products, yet many of their properties are still the subject of controversy. The flow-driven self-organization of the crystals at the air–water interface was analyzed to gain understanding of how their properties might influence their dynamic behavior and exploitation in applications.

■ EXPERIMENTAL DETAILS

Crystals of small-molecule amphiphiles including sodium salicylate, salicylic acid, *o*-acetylsalicylic acid, bromobenzaldehyde, methylhydroxy benzoate, nitrophenyl acetate, and benzoyl peroxide were used as purchased from Sigma. Aspirin crystals (Sigma A2093) were selected for detailed analysis because of their slow hydrolysis and dissolution rate compared with the others. Crystals of average mass of 1 ± 0.2 mg were chosen to facilitate analysis of the motion and interaction of a small number of crystals by digital photography. Larger crystals

Received: May 31, 2013

Revised: September 9, 2013

sank immediately and smaller crystals (<0.1 mg) exhibited much faster motion. Individual crystals were weighed and photographed for characterization before their use in experiments. We selected crystals of similar size with an elliptic shape ($1.5 \pm 0.1 \times 0.8 \pm 0.1 \times 0.6 \pm 0.1$ mm³) for the determination of the speed at different ion concentrations as we found that both of these factors affected the speed and path of motion. No discernible change in the shape and size of the crystals was observed during the first few minutes of an experiment. The solutions were prepared with distilled, deionized water and H₂SO₄, NaOH, NaCl, or NaH₂PO₄/Na₂HPO₄ was added to give the indicated pH or concentration. The pH of a solution was determined using a pH meter.

A side view of an aspirin crystal at the air–water interface was obtained in a thin reaction cell (W30 mm, H25 mm, D5 mm) with solution of depth 8 mm. Experiments on the motion of aspirin crystals were performed in a 5 cm diameter, thermostatted perspex Petri dish ($T = 20$ °C) containing solution of depth 8 mm, total volume 16 mL. The crystal motion was affected by the presence of any contaminants in the Petri dishes or changes in air temperature or in the depth of the solution. The crystals were illuminated using a strip-light (LED, white) surrounding the perimeter of the Petri dish. A series of images was obtained using a CCD camera with frame rate 12 s^{-1} and processed using Matlab script written in-house, except for Figure 1b, where a DSLR camera equipped with macro lens and a floodlight mounted on opposite sides of the Petri dish at 45° to the monitored interface were used.

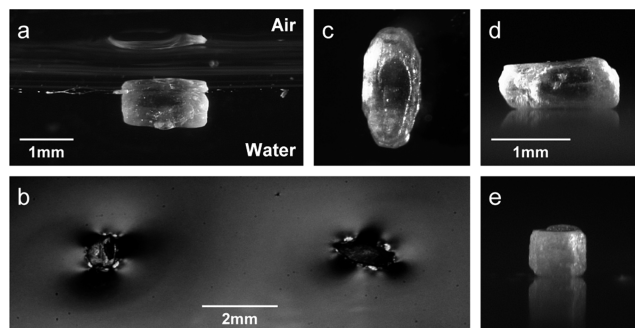


Figure 1. (a) Side view of an aspirin crystal suspended at the air–water interface. (b) Surface deformations generated by two crystals in motion at the air–water interface where the dark regions correspond to depressions in the surface. (c–e) Ellipsoid shape and size of typical aspirin crystals used in experiments.

The front speed was determined from the extracted coordinates of a crystal's center of mass as a function of time. The time-average speeds from six experiments were used to determine the average and standard deviation of the speeds of a crystal for a particular solution composition. In experiments on groups of crystals, the sum of the separation of crystal pairs was calculated from:

$$\sum_{i=1}^N \sum_{j=i+1}^N d_{ij} \quad (1)$$

where N = total number of crystals and d_{ij} is the distance between the i th and j th crystals' center of mass.

RESULTS AND DISCUSSION

The position and capillary profile of a solid object at the air–water interface are determined by its weight and shape and the surface free energies related to the liquid–gas, liquid–solid, and solid–gas interfaces.²³ Aspirin crystals are denser than water (1.4 g/mL) but are nevertheless trapped at the air–water interface (Figure 1a). The crystals were almost completely submerged and sank to the bottom of the dish when pushed below the surface. The surface deformations shown in Figure 1b arise from a combination of the crystal's size, ellipsoid shape²⁴ (Figure 1c–d), and structural anisotropy.²⁵ The hydrophilicity of the facets of large (>2 cm) aspirin crystals was found to be $(011) > (100) > (001)$ with the hydrophobicity of the major (001) facet arising from the exposure of the phenyl groups.²⁶ The crystals used in the experiments reported here may contain intergrowth domains of two polymorphs and have patchy wetting properties/surface energies that are difficult to characterize.²⁷ The surface profile is further complicated by the dissolution (solubility = 3 g/mL) and hydrolysis of aspirin; however, these processes are relatively slow compared with the time scale of observations discussed here.^{28,29} The hydrolysis product at high pH, sodium salicylate, is a hydrotrope and weakly surface active.³⁰

Placed in a Petri dish of water, crystals move on the surface with average speeds on the order of 10 mm s^{-1} . Paths and speeds of the crystals in time are shown in Figure 2. The

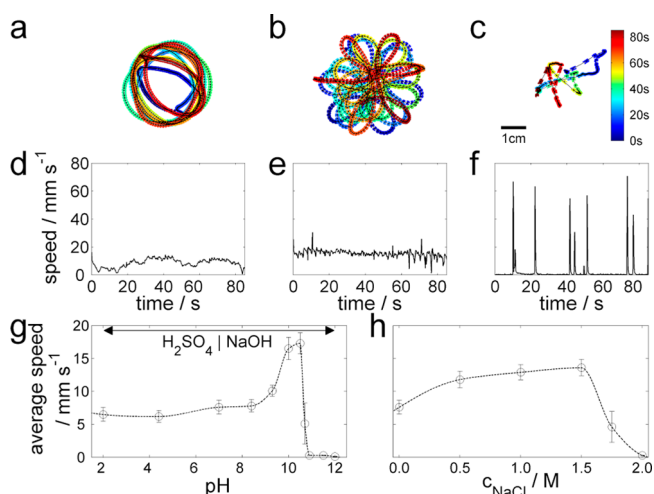


Figure 2. Paths traced (a–c) and speed–time plots (d–f) of aspirin crystals at the aqueous–air interface with the addition of H₂SO₄ or NaOH to give pH (a,d) 5; (b,e) 10; and (c,f) 11. Average speed of crystals as a function of (g) pH and (h) concentration of NaCl.

magnitude of the average speed is typical of objects driven by Marangoni flows.⁸ Aspirin shares the short-chain hydrophobic/hydrophilic properties of its hydrotropic hydrolysis product and thus lowers the surface tension as it slowly dissolves. The resultant surface-tension gradient gives rise to a hydrodynamic flow that propels the crystals. All other crystals we investigated (see Experimental Details) consisted of benzene rings with hydrophilic side chains and exhibited self-motion, whereas surfactant crystals such as cetyl trimethylammonium bromide (CTAB) did not. Weak surface activity (or a lack of rapid surface saturation) is therefore important to generate a gradient in surface tension around a dissolving substance, and crystals of

small amphiphiles can be added to the list of chemical skaters with autonomous motion driven by a Marangoni flow.

The motion of the crystals was influenced by the presence of other ions. The path of the crystals was mainly circular when the pH of the solution was below 7 by addition of H_2SO_4 (Figure 2a). However, some crystals reversed their direction of motion or displayed more complex paths. When the pH was increased to 10 by addition of NaOH, the average speed of the crystals increased and hypocycloid paths were observed (Figure 2b). At pH 11, the crystals displayed short bursts of high speed (up to 70 mm s^{-1}), followed by periods of slow drifting (Figure 2c). Only slow drifting motion of the crystals was observed at pH 12.

The trend of the average speed increasing to a maximum before falling close to zero (Figure 2d) is not solely a result of the increasing pH: we observed the same trend with increasing phosphate buffer strength at pH 7 (over 0.2 M), decreasing temperature (down to 10°C at pH 10), or increasing ionic strength by addition of NaCl to water (Figure 2e). The motion can be instantly stopped by addition of surfactant (e.g., CTAB), addition of alcohol, or use of sodium salicylate solution (3 M).

It is impossible to separate the surface-tension changes upon addition of chemicals or changes in temperature from other factors in these experiments; for example, the hydrolysis rate is also affected by the change in pH. However, the change in surface tension is the common factor influencing the speed of the crystals: a decrease in temperature leads to an increase in surface tension, and addition of inorganic salts, NaOH, and H_2SO_4 (but not other acids) also leads to an increase in surface tension correlated with a depletion of ions at the surface.³¹ Organic amphiphiles decrease the surface tension and have an enhanced surface concentration. The results suggest there is a bounded range of surface tensions for which motion of these chemical skaters is possible.

The origin of the short bursts of high-speed motion at pH 11 is not clear, but periodic motion has also been observed with camphor boats and gel particles.^{32,33} This motion may be related to an oscillatory Marangoni instability³⁴ observed during transfer of a drop of surfactant into an aqueous phase. Above a critical value of the surface tension, there is a sudden drop in surface tension correlated with convective transport of the surfactant and gradual recovery correlated with diffusive transport of the surfactant.

The path traced by chemical skaters is partially dictated by their shape, and elliptic particles move linearly, short axis first.³⁵ Aspirin crystals also tend to move short axis first, but their path is affected by capillary interactions with the meniscus at the walls of the Petri dish. The dominant interaction of aspirin crystals with the meniscus was repulsive, hence the crystals followed circular (lower speeds) or hypocycloid paths (higher speeds) and the burst motion was confined to the center of the Petri-dish.

In contrast with experiments with camphor,^{14,36,37} aspirin crystals displayed complex interactions with each other that sometimes led to the formation of moving dimers or larger groups. At pH <10, the collisions between crystals could be sticky, resulting in the instant attachment of crystals, or bouncy, where the crystals collided a number of times in close proximity before forming a dimer. Deflection and reversal of motion was also observed in certain cases when the crystals approached each other.

The interaction of two crystals leading to stable dimer formation at low pH is illustrated in Figure 3. A larger crystal

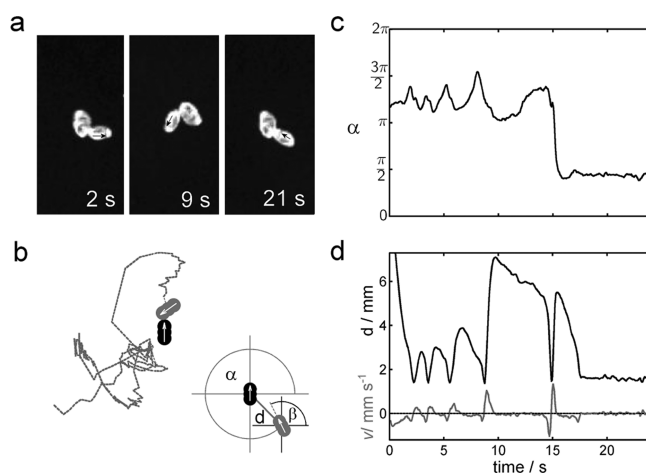


Figure 3. Pair of crystals underwent a series of collisions at the aqueous–air interface (pH 1) before finding a favorable orientation where they subsequently moved as a dimer. (a) Images of the two crystals colliding at the indicated times. (b) Left: The path of the larger crystal (gray) relative to the fixed frame of reference given by the smaller crystal (black). Right: The angle α and distance d between the two crystal centers give the polar coordinates of the larger crystal relative to the smaller crystal, and the angle β gives the orientation of the larger crystal. (c) Angle α in time. (d) Distance and velocity in time. An accompanying movie of the crystals is available in the Supporting Information.

approaches a smaller crystal and a number of collisions ensue. At each collision the crystals form a dimer with a specific orientation: in Figure 3a, the first, fourth, and sixth collisions are shown. The path of the larger crystal is indicated in Figure 3b as well as various measures related to the crystal motion. When the crystals are within 1 mm of each other, there is a rapid decrease in their separation (and accompanying negative velocity), followed by an equally rapid increase soon after they touch (Figure 3d). Following the fifth collision, the larger crystal changes quadrant with $\alpha \approx \pi$ to $\pi/2$ and orientation from $\beta = 0$ to π (shown online); at this point the crystals find a stable orientation, and the two subsequently move as a dimer for the rest of this experiment.

Groups of attached crystals underwent both translational and rotational motion. Rotational motion tended to dominate when crystals aligned end-to-end, as illustrated in Figure 4. In this case, the crystal pair (Figure 4a) underwent fast rotation until a third crystal joined the group, and the rotation frequency was significantly reduced. The paths traced by the three crystals are shown in Figure 4b, where the tight corkscrew path of the two crystals (red and green) unwinds with the addition of the third crystal (blue).

The nature of the interaction was also affected by the pH. With the pH <10, dimers or larger groups formed and disbanded during the course of the experiment (Figure 5a), reflected in the fluctuating sum of the separation of crystal pairs in time (Figure 5c). When the pH was increased to 11 (Figure 5b), the crystals drifted toward each other (and the center of the Petri dish); however, no stable dimers were formed. In contrast with Figure 5c, the separation plot in Figure 5d consisted of slow decay when the crystals approached each other and sharp increases when the crystals displayed bursts of motion. At pH 12, the crystals drifted slowly together (again toward the center of the dish) until they were within several millimeters of each other; they then accelerated toward each

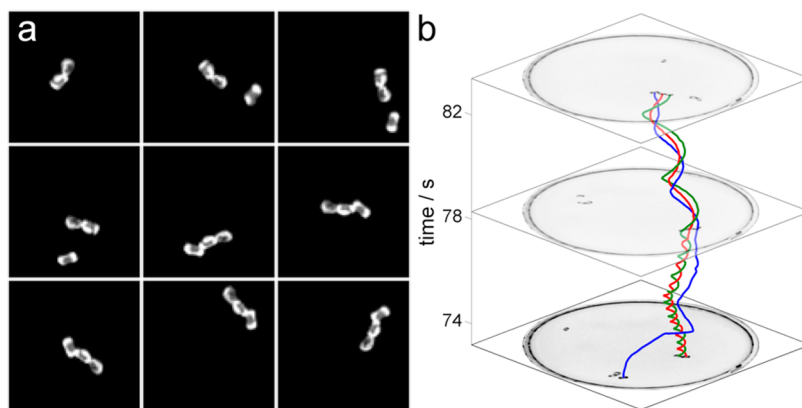


Figure 4. Rotational motion of crystal groups at the water–air interface (pH 6.5): (a) a series of images ($1.3 \times 1.3 \text{ cm}^2$ taken at 1.3 s intervals) in which a third crystal joins a dimer of crystals aligned end-to-end. (b) Successive images of the Petri dish (5 cm diameter) and the paths of the three aspirin crystals forming a rotating trimer (lines). An accompanying movie of the crystals is available in the Supporting Information.

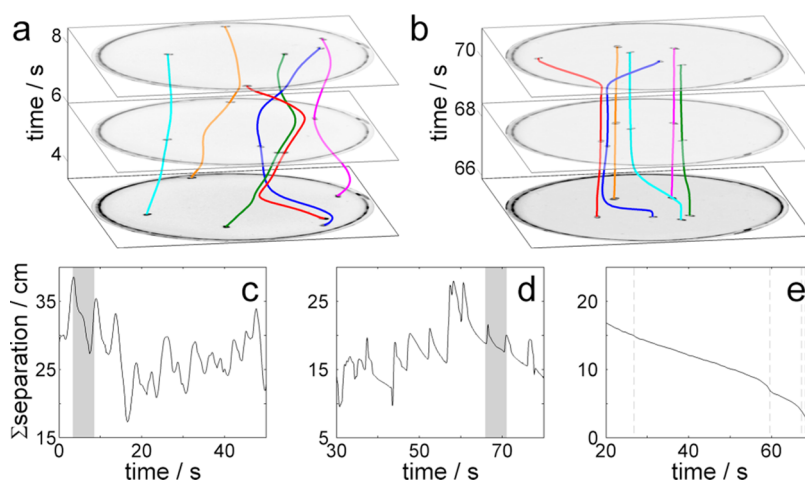


Figure 5. Successive images of the Petri dish (5 cm diameter) and the paths of six aspirin crystals (lines) at the air–water interface at pH (a) 7 and (b) 11. (c–e) Sum of the separation of all crystal pairs in time with pH (c) 7, (d) 11, and (e) 12. The highlighted regions in panels c and d correlate with the images shown in panels a and b. Accompanying movies of the crystal motion are available in the Supporting Information.

other. Groups of two or three crystals eventually coalesced to form one large group. A typical sum of the separations plot is shown in Figure 5e.

The behavior of groups of crystals can be explained by a combination of capillary interactions and Marangoni effects, although electrostatic interactions during collisions cannot be ruled out.²² Anisotropic particles have capillary profiles that can lead to alignment in specific orientations.³⁸ The capillary profile of the dense aspirin particle (Figure 1c) shows dips and rises that may result in attractive or repulsive interactions depending on the orientation of the crystals. Some aspirin crystals are capable of turning and realigning in a series of bouncy collisions as the complex surface deformations in the vicinity of each crystal result in sharp changes between like and unlike interactions. Like interactions lead to the formation of dimers; however, the attractive forces are often overcome by surface flows as a result of the Marangoni effect in the vicinity the crystals. Convective Marangoni flows result in the dominance of short-range repulsive interactions in the case of camphor-loaded particles, which are buoyant and show no evidence of capillary attractions.¹⁴

At pH 11, the burst motion that is probably governed by a periodic Marangoni instability dominates. Thus when two crystals approach each other, the concentration gradient from

the two crystals results in a large convective flow. At pH 12, the crystals are no longer subject to convective surface flows; then, capillary interactions dominate, leading to the formation of stable groups of crystals.

Much attention has been paid to the possibility of combining autonomous motion and self-assembly of nano- to millimeter sized particles with potential applications in materials science of drug delivery.³⁹ Possibly the first example of this involved the creation of moving dimers of mm-sized disks through bubble propulsion from a catalytic reaction coupled with capillary interactions.⁴⁰ These experiments were inspired by the collective behavior of swimming organisms such as bacteria. Janus particles that achieve motion by diffusiophoresis^{41,42} have also been assembled into dimers displaying more complex motion.^{43,44} Hydrodynamic flows driven by Marangoni effects were tuned by using shaped gel-particles loaded with camphor resulting in lattices of stationary particles or moving swarms.^{14,37} There is increasing interest in directing the assembly of particles by tuning their shape and chemical structure, and hence their capillary profile.^{38,45,46}

No attempt was made to control the crystal structure in this work, but techniques might be used to grow crystals of small amphiphile molecules tailored for specific interactions and containing insoluble elements. Cargo-carrying amphiphilic

crystals with designed anisotropy may have applications in the directed assembly of objects at interfaces. It will be of interest to determine whether the flow-driven self-organization arising with millimeter-sized aspirin crystals is possible with micro- to nanoscale crystals. Sufficient numbers of crystals would provide the surface activity required for Marangoni flows; however, the capillary profiles that lead to oriented interactions between crystals arise from a combination of the crystals' size, shape, and chemical properties, and these interactions may become less significant as the size of the crystal is decreased. This will be the subject of further investigation.

CONCLUSIONS

The mechanisms of motion and interaction of particles are of interest for dynamic self-assembly of materials and devices as well as for the investigation of collective behaviors in biology. Here we have demonstrated that millimeter-sized aspirin crystals show motion and complex interactions at the air–water interface driven by a combination of Marangoni effects from weak surface activity and capillarity. The speed of the crystals was influenced by the presence of ions in solution, and motion occurred within a bounded range of surface tensions. The bursts of speed observed at high pH were proposed to arise from a periodic Marangoni instability. Capillary interactions resulted in the formation of dimers or larger groups of crystals that also underwent motion.

ASSOCIATED CONTENT

Supporting Information

Experimental details and accompanying movies for Figures 3–5 showing motion and interaction of aspirin crystals. Figure 3: Interaction of a pair of crystals leading to dimer formation at the aqueous–air interface (pH 1). Figure 4: Rotational motion of groups of crystals at air–water interface (pH 6.5). Figure 5a: Motion of six crystals at pH 7 and sum of the separation of all crystal pairs in time. Figure 5b: Motion of six crystals at pH 11 and sum of the separation of all crystal pairs in time. Figure 5c: Motion of six crystals at pH 12 and sum of the separation of all crystal pairs in time. This material is available free of charge via the Internet at <http://pubs.acs.org>.

AUTHOR INFORMATION

Corresponding Author

*E-mail: A.F.Taylor@leeds.ac.uk. Fax: (+)44 113 3436565.

Notes

The authors declare no competing financial interest.

ACKNOWLEDGMENTS

T.B. was supported by a Marie Curie International Incoming Fellowship (grant agreement PIFI-GA-2010-274677).

REFERENCES

- (1) Israelachvili, J. N. *Intermolecular and Surface Forces*, 3rd ed.; Elsevier Academic Press: San Diego, 2011.
- (2) Myers, D. *Surfaces, Interfaces, And Colloids: Principles and Applications*; Wiley-VCH: New York, 1999.
- (3) Fan, Y. B.; Chen, X.; Yang, L. J.; Cremer, P. S.; Gao, Y. Q. On the Structure of Water at the Aqueous/Air Interface. *J. Phys. Chem. B* **2009**, *113*, 11672.
- (4) Stipkin, I. V.; Weeraman, C.; Pieniazek, P. A.; Shalhout, F. Y.; Skinner, J. L.; Benderskii, A. V. Hydrogen bonding at the water surface revealed by isotopic dilution spectroscopy. *Nature* **2011**, *474*, 192.
- (5) Verreault, D.; Hua, W.; Allen, H. C. From Conventional to Phase-Sensitive Vibrational Sum Frequency Generation Spectroscopy: Probing Water Organization at Aqueous Interfaces. *J. Phys. Chem. Lett.* **2012**, *3*, 3012.
- (6) Keller, J. B. Surface tension force on a partly submerged body. *Phys. Fluids* **1998**, *10*, 3009.
- (7) Scriven, L. E.; Sternling, C. V. Marangoni effects. *Nature* **1960**, *187*, 186.
- (8) Nakata, S.; Iguchi, Y.; Ose, S.; Kuboyama, M.; Ishii, T.; Yoshikawa, K. Self-rotation of a camphor scraping on water: New insight into the old problem. *Langmuir* **1997**, *13*, 4454.
- (9) Hanczyc, M. M.; Toyota, T.; Ikegami, T.; Packard, N.; Sugawara, T. Fatty acid chemistry at the oil-water interface: Self-propelled oil droplets. *J. Am. Chem. Soc.* **2007**, *129*, 9386.
- (10) Bain, C. D.; Burnetthall, G. D.; Montgomerie, R. R. Rapid motion of liquid-drops. *Nature* **1994**, *372*, 414.
- (11) Chaudhury, M. K.; Whitesides, G. M. How to make water run uphill. *Science* **1992**, *256*, 1539.
- (12) Pimienta, V.; Brost, M.; Kovalchuk, N.; Bresch, S.; Steinbock, O. Complex Shapes and Dynamics of Dissolving Drops of Dichloromethane. *Angew. Chem., Int. Ed.* **2011**, *50*, 10728.
- (13) Bush, J. W. M.; Hu, D. L. Walking on water: Bioloocomotion at the interface. *Annu. Rev. Fluid Mech.* **2006**, *38*, 339.
- (14) Soh, S.; Branicki, M.; Grzybowski, B. A. Swarming in Shallow Waters. *J. Phys. Chem. Lett.* **2011**, *2*, 770.
- (15) Maillard, M.; Motte, L.; Ngo, A. T.; Pileni, M. P. Rings and hexagons made of nanocrystals: A Marangoni effect. *J. Phys. Chem. B* **2000**, *104*, 11871.
- (16) Kralchevsky, P. A.; Nagayama, K. Capillary interactions between particles bound to interfaces, liquid films and biomembranes. *Adv. Colloid Interface Sci.* **2000**, *85*, 145.
- (17) Denkov, N. D.; Velev, O. D.; Kralchevsky, P. A.; Ivanov, I. B.; Yoshimura, H.; Nagayama, K. 2-Dimensional crystallisation. *Nature* **1993**, *361*, 26.
- (18) Pieranski, P. Two-dimensional interfacial colloidal crystals. *Phys. Rev. Lett.* **1980**, *45*, 569.
- (19) Bowden, N.; Terfort, A.; Carbeck, J.; Whitesides, G. M. Self-assembly of mesoscale objects into ordered two-dimensional arrays. *Science* **1997**, *276*, 233.
- (20) Bowden, N.; Choi, I. S.; Grzybowski, B. A.; Whitesides, G. M. Mesoscale self-assembly of hexagonal plates using lateral capillary forces: Synthesis using the “capillary bond”. *J. Am. Chem. Soc.* **1999**, *121*, 5373.
- (21) Cappella, B.; Dietler, G. Force-distance curves by atomic force microscopy. *Surf. Sci. Rep.* **1999**, *34*, 1.
- (22) Eastoe, J.; Hatzopoulos, M. H.; Dowding, P. J. Action of hydrotropes and alkyl-hydrotropes. *Soft Matter* **2011**, *7*, S917.
- (23) Ivanov, I. B.; Kralchevsky, P. A.; Nikolov, A. D. Film and line tension effects on the attachment of particles to an interface. *J. Colloid Interface Sci.* **1986**, *112*, 97.
- (24) Cavallaro, M., Jr.; Botto, L.; Lewandowski, E. P.; Wang, M.; Stebe, K. J. Curvature-driven capillary migration and assembly of rod-like particles. *Proc. Natl. Acad. Sci. U. S. A.* **2011**, *108*, 20923.
- (25) Bond, A. D.; Boese, R.; Desiraju, G. R. On the polymorphism of aspirin. *Angew. Chem., Int. Ed.* **2007**, *46*, 615.
- (26) Heng, J. Y. Y.; Bismarck, A.; Lee, A. F.; Wilson, K.; Williams, D. R. Anisotropic surface chemistry of aspirin crystals. *J. Pharm. Sci.* **2007**, *96*, 2134.
- (27) Varughese, S.; Kiran, M. S. R. N.; Solanko, K. A.; Bond, A. D.; Ramamurty, U.; Desiraju, G. R. Interaction anisotropy and shear instability of aspirin polymorphs established by nanoindentation. *Chem. Sci.* **2011**, *2*, 2236.
- (28) Edwards, L. J. The dissolution and diffusion of aspirin in aqueous media. *Trans. Faraday Soc.* **1951**, *47*, 1191.
- (29) Edwards, L. J. The hydrolysis of aspirin. *Trans. Faraday Soc.* **1952**, *48*, 696.
- (30) Balasubramanian, D.; Srinivas, V.; Gaikar, V. G.; Sharma, M. M. Aggregation behaviour of hydrotropic compounds in aqueous solution. *J. Phys. Chem.* **1989**, *93*, 3865.

- (31) Jungwirth, P.; Tobias, D. J. Specific ion effects at the air/water interface. *Chem. Rev.* **2006**, *106*, 1259.
- (32) Sharma, R.; Chang, S. T.; Velev, O. D. Gel-Based Self-Propelling Particles Get Programmed To Dance. *Langmuir* **2012**, *28*, 10128.
- (33) Nakata, S.; Iguchi, Y.; Ose, S.; Ishii, T. pH-sensitive self-motion of a solid scraping on an aqueous phase. *J. Phys. Chem. B* **1998**, *102*, 7425.
- (34) Lavabre, D.; Pradines, V.; Micheau, J. C.; Pimienta, V. Periodic Marangoni instability in surfactant (CTAB) liquid/liquid mass transfer. *J. Phys. Chem. B* **2005**, *109*, 7582.
- (35) Kitahata, H.; Iida, K.; Nagayama, M. Spontaneous motion of an elliptic camphor particle. *Phys. Rev. E* **2013**, *87*.
- (36) Nakata, S.; Doi, Y.; Kitahata, H. Synchronized sailing of two camphor boats in polygonal chambers. *J. Phys. Chem. B* **2005**, *109*, 1798.
- (37) Soh, S.; Bishop, K. J. M.; Grzybowski, B. A. Dynamic self-assembly in ensembles of camphor boats. *J. Phys. Chem. B* **2008**, *112*, 10848.
- (38) Botto, L.; Lewandowski, E. P.; Cavallaro, M., Jr.; Stebe, K. J. Capillary interactions between anisotropic particles. *Soft Matter* **2012**, *8*, 9957.
- (39) Paxton, W. F.; Sundararajan, S.; Mallouk, T. E.; Sen, A. Chemical locomotion. *Angew. Chem., Int. Ed.* **2006**, *45*, 5420.
- (40) Ismagilov, R. F.; Schwartz, A.; Bowden, N.; Whitesides, G. M. Autonomous movement and self-assembly. *Angew. Chem., Int. Ed.* **2002**, *41*, 652.
- (41) Howse, J. R.; Jones, R. A. L.; Ryan, A. J.; Gough, T.; Vafabakhsh, R.; Golestanian, R. Self-motile colloidal particles: From directed propulsion to random walk. *Phys. Rev. Lett.* **2007**, *99*.
- (42) Ke, H.; Ye, S.; Carroll, R. L.; Showalter, K. Motion Analysis of Self-Propelled Pt-Silica Particles in Hydrogen Peroxide Solutions. *J. Phys. Chem. A* **2010**, *114*, 5462.
- (43) Ebbens, S.; Jones, R. A. L.; Ryan, A. J.; Golestanian, R.; Howse, J. R. Self-assembled autonomous runners and tumblers. *Phys. Rev. E* **2010**, *82*.
- (44) Valadares, L. F.; Tao, Y. G.; Zacharia, N. S.; Kitaev, V.; Galembeck, F.; Kapral, R.; Ozin, G. A. Catalytic Nanomotors: Self-Propelled Sphere Dimers. *Small* **2010**, *6*, 565.
- (45) Grzelczak, M.; Vermant, J.; Furst, E. M.; Liz-Marzan, L. M. Directed Self-Assembly of Nanoparticles. *ACS Nano* **2010**, *4*, 3591.
- (46) Boker, A.; He, J.; Emrick, T.; Russell, T. P. Self-assembly of nanoparticles at interfaces. *Soft Matter* **2007**, *3*, 1231.